International Journal of Thermofluid Science and Technology (2024)
Volume 11, Issue 2, Paper No. 110203
https://doi.org/10.36963/IJTST.2024110203
Research Article

Thermal-hydrodynamic analysis for internally finned tubes: Experimental, numerical and performance evaluation study

O. H. Salem*, Ahmed Hegazy, K. Yousef

Department of Mechanical Power Engineering, Faculty of Engineering, Menoufia University, Shebin El-Kom, 32511, Egypt

ATICLE INFO

Received: 06 Mar. 2024;
Received in revised form:
26 Apr. 2024;
Accepted: 20 May 2024;
Published online:
28 May 2024

Keywords:
continuously finned tube
thermal-hydrodynamic performance
heat transfer applications

ABSTRACT

The characteristics of heat transfer and fluid flow of an internally continuously finned tube were studied, experimentally and numerically, and a performance evaluation study was conducted. The numerical results were validated with the current experimental data as well as other published data, with a maximum deviation of 4.65%. The effect of different key parameters like fin height, number of fins, and fin thickness on the thermal-hydrodynamic performance was studied. The study reveals that increasing both fin height, which is the most effective parameter, and number of fins raises the heat transfer coefficient and friction factor values, but fin thickness negligibly affects the performance. Notably, the average heat transfer coefficient and friction factor values rise by 40.92 % and 18.4 %, respectively, if the fin height to diameter ratio is increased from 0.1786 to 0.4018, and by 35.4 % and 13.5 %, respectively, if the number of fins is increased from 2 to 6, compared to smooth tubes under a mass flow rate of 0.3 kg/s. Furthermore, the thermal enhancement factor, which is the ratio between the heat transfer coefficient and friction factor for the enhanced tube as opposed to the smooth one, increases by 33.27%, 48.64%, and 8.71% if the fin height, number of fins, and fin thickness increase by 125%, 300%, and 200%, respectively, under constant mass flow rate condition. While the thermal enhancement factor decreases by 22.89%, 74.53%, and 7.92% if the fin height, number of fins, and fin thickness increase by 125%, 300%, and 200%, respectively, under constant pressure drop condition. In the case of constant pumping power condition, the thermal enhancement factor hovers around unity for fin height and thickness, and it decreases by 23.89% if the number of fins increases by 300%.

1. Introduction

There is an increasing demand for high-performance heat exchangers that can effectively save waste energy and enhance the energy recovery process [1-3]. Such heat exchangers can be very beneficial in many fields of engineering such as power plants,

*Corresponding e-mail: sciencehub25@gmail.com (O. H. Salem)

Nomenclature

A	area, m^2	v	mean velocity, $m.s^{-1}$
C_p	specific heat, $J.kg^{-1}.K^{-1}$	x	axial location, m
d	internal tube diameter, m	*Greek symbols*	
f	friction factor	μ	dynamic viscosity, Pa. s
H	fin height, m	ρ	density, $kg.m^{-3}$
h	heat transfer coefficient, $W.m^{-2}.K^{-1}$	*Subscripts*	
k_{th}	thermal conductivity, $W.m^{-1}.K^{-1}$	avg	average
L	tube length, m	c	cross-section
m	mass flowrate, $kg.s^{-1}$	f	finned section
N	number of fins	h	hydraulic
Nu	Nusselt number	i	inlet
Pr	Prandtl number	m	mean
p	pressure, Pa	o	outlet
q	heat flux, $W.m^{-2}$	s	surface
Re	Reynolds number	t	turbulent
T	temperature, K	w	wall
t	fin thickness, m	x	local

chemical processes, petroleum industries, evaporation and condensation processes, and heating and cooling processes [4-6]. To make such devices more efficient, they are integrated with thermally improved tubes that can be enhanced by whether the active methods such as jet impact, surface vibration, electrostatic field, and electromagnetic field strengthening [7-9], or the passive methods [10-11], which require no external power, like extended surfaces, which are simply called fins, and the utilization of nanofluids [12-15]. Regarding the passive methods, the use of nanofluids is not a good choice due to the stability and the other issues associated with the use of nanofluids [16-17]. So, the use of fins, whether on the external surface (externally finned tubes) or on the internal one (internally finned tubes) [18], as a passive method for heat transfer enhancement attracted many scholars' attention due to the high heat transfer rates and area [19-20].

Many scholars studied the issue of optimizing the finned surfaces' shapes to increase thermal efficiency under different conditions. Analytical and numerical studies to assess the performance of laminar fully developed internally finned tubes have been conducted [21-23]. It has been found that the secondary flow is one of the important features of the flow in internally finned tubes as it affects their thermal performance. These results were supported by numerical studies [24-25], their aim was to assess the performance of internally finned tubes with different wavy fins with S, V, and Z, sinusoidal, and interrupted wavy shapes. It was found that the secondary flow is relatively strong at the lower wall of the inside channel. Furthermore, the Nusselt number of the Z-shape fins is the highest, while the Nusselt number and the friction factor of the V-shape fins are the lowest. Additionally, it was found that fins stamped out with ellipsoidal protrusions in a heat exchanger enhance its thermal performance because these protrusions can substantially improve the intensity of secondary flow and enhance heat transfer [26]. Also, the performance of other fin shapes has been studied numerically and experimentally [27-28], including rectangular, saw, T-shape (studied also in [29]), and trapezoidal shape. It was found that the minimum wall temperature occurs at fin height to diameter ratio equals 0.257, which is less than what was mentioned in [29], also the T-shaped fin has a higher heat transfer rate compared to other shapes not as mentioned in [29]. Numerical studies for the optimization of heat transfer inside internally finned tubes have been conducted in [30-32]. It

was found that the presence of eddies due to fins' existence increases the apparent viscosity and the turbulence effect. Zeitoun et al. [33] studied numerically the heat transfer for laminar flow in internally finned pipes with different fin heights. They revealed that if the height of one fin gets shorter, its contribution to heat transfer is reduced. A numerical investigation was conducted to assess the performance of continuously finned tubes under different flow conditions [34]. It was found that the fin height is the most effective parameter on the thermal performance of the finned tube. Also, the heat transfer coefficient is enhanced 9 times, and the friction coefficient rises 2 times in value compared to the smooth one.

Recently, many scholars began to assess the reliability of using finned tubes in new fields including enhanced heat exchangers, renewable energy, phase change material science, and nanofluid science. Tabassum et al. [35] conducted numerical investigations of melting a paraffin wax placed inside a circular concentric finned annulus for thermal storage. They found that the Nusselt number and the total energy stored increased in the finned annulus compared to the finless one. Also, they found that extending the fin height to 50% increases the energy storage by 33.05%. Zhang et al. [36] conducted a numerical and experimental study to assess the performance of a finned tube heat exchanger with phase change material (organic PCM A27). They found that the time of melting and solidification can be reduced by 46% and 35%, respectively, by improving the thermal conductivity of the PCM. Heydari et al. [37] conducted a numerical investigation to assess the effect of semi-attached and offset mid-truncated ribs on the heat transfer performance of a triangular microchannel, through which the nanofluid water-TiO2 flows. They found that the implementation of these ribs increases the Nusselt number and the total thermal efficiency but decreases the friction coefficient. Sun et al. [38] carried out a numerical study to optimize the thermo-hydraulic behavior of a linear Fresnel solar reflector integrated with spiral finned tubes. They found that the spiral fin can increase the fluid temperature and the conversion efficiency of the receiver, Also, they found that the Nusselt number of the receiver tube and the thermal performance factor are enhanced by 29% and 116%, respectively, compared to the finless one. Hassan et al. [39] executed an experimental study to assess the performance of a heat exchanger integrated with inner finned tubes. They found that the Nusselt number, the heat transfer coefficient, and the effectiveness are enhanced by 95%, 53%, and 127%, respectively, compared to the finless case at the same Reynolds number. However, the friction factor in the finned case increases by 63% at a low Reynolds number compared to the smooth one. Guo et al. [40] conducted an experimental and numerical study to assess the performance of vertical shell-and-tube thermal energy storage tubes with fins of positive and negative gradient height. They found that the negative gradient fins perform better than the positive gradient fins compared to the uniform ones.

In the present work, an experimental, numerical, and performance evaluation analysis has been carried out to assess the thermal-hydrodynamic performance for turbulent flow regime inside internally continuously finned tubes. Detailed experimental work has been conducted, considering every right step to guarantee highly reliable experimental data. In addition, this experimental study has been extended with a CFD modeling to obtain the geometrical parameters' effect on the performance of the continuously finned tubes with a good deep explanation, as well as the effect rank of each geometrical parameter under different operating conditions. Furthermore, a thermo-hydrodynamic evaluation study has been conducted, based on a new concept and under three different constraints, namely constant mass flow rate, constant pressure drop, and constant pumping power, to get a precise evaluation of such tubes and to reveal the goodness of using these tubes inside thermal devices. Additionally, precise, to some extent, equations have been generated to get different thermal and hydrodynamic parameters of such tubes and these equations have been compared with other well-known equations to show their

validity. This work can be considered as a cornerstone of using the internally continuously finned tubes and how they can improve or not the performance of any heat transfer device integrated with them.

2. Experimental method

2.1 Experimental test-rig

A layout of the designed and constructed system in this work is shown in Fig. 1. It consists mainly of a water pumping cycle, heating mechanism, and measuring instruments. Water is drawn from the tank (1) by using a constant speed centrifugal pump (3), which serves to transmit water through a delivery valve (2) connected to a calibrated rotameter (4) to measure the circulated water flow rate. Water is directed to flow through a 60 cm long and 5.6 cm inner diameter pipe (d) just before entering the flow conditioner (5), which has a 40 cm length and 5.6 cm inner diameter with very small diameter (3 mm) tubes inside it to ensure that the flow is uniform at the conditioner outlet. The water flow is then directed into the test section (6) and finally discharged to the outside. The whole system is designed so that the test section has a lower level compared to its inlet and outlet sections to ensure that the whole test section is continuously filled with water.

Two test tubes are made of galvanized iron to make them corrosion-resistant with a 6 cm outer diameter and 5.6 cm inner diameter. This tube diameter is chosen to be close to the real dimensions of tubes inside a heat exchanger used in a major process. One of the test tubes is fitted with 2 fins, and the other is supplied with 4 fins. To provide the two tubes with the fins in the correct positions, two slots are cut in one tube and 4 ones are cut in the other, along the whole finned sections of the tubes. The slots have a width of 0.6 cm, and they start 50 cm after the inlet finless section for the continuously finned tubes. The fins, made of iron, are inserted into these slots, and welded to the tubes' surfaces. All long fins are 1.5 cm in height and 0.6 cm thick. This operation, to some extent, ensures that the tube surface and the fins are merged to avoid thermal contact resistance and to ensure that there are no welding residues on the inner surface of the tubes. This may help avoid any effect on the fluid flow. All tested tubes are 100 cm long with 50 cm finless length before the fins and 10 cm after them. The heating mechanism used in the test rig is composed of an ohmic resistance nichrome tape (0.3 cm width, 0.02 cm thickness, and 2.36 ohm/m) is wrapped uniformly around the outer surface of the tube. The output power from the heater is controlled by using a variable voltage transformer (STACO type) (7), which provides a uniform heat flux along the tube surface. A 0.15 cm thick layer of asbestos is used to cover the outer surface of the tube to act as an electrical insulation. The outer surface of the heater is electrically and thermally insulated using another 0.15 cm thick layer of asbestos cloth, a layer of fiberglass, a layer of fiber ceramic blanket with 3 cm thickness, and a layer of compressed asbestos fiber (Superlite 111). The thermal insulation covers the whole test section except the first 50-cm length while the heater tape covers the whole test section except the first 50-cm section and the 10-cm finless section at the tube end. Fig. 2 shows the different thermal and electrical insulation layers applied to the tested tube.

T-type calibrated thermocouples (8) of 0.05 cm head diameter embedded at the tips of all fins circumferentially and axially along the continuously finned tubes. For the tube fitted with 4 fins, 2 thermocouples are used to measure the fins' tips temperatures and 2 thermocouples to measure the wall temperatures, while for the tube fitted with 2 fins, 2 thermocouples are used to measure the temperatures of the fin tips, and one thermocouple to measure the wall temperature. Another 10 thermocouples of T-type are distributed uniformly at different radial positions at the tube outlet to measure the outlet fluid temperature. The output from thermocouples is recorded by a data acquisition (NI cDAQ-9174) (9), which is connected to a computer (10) using lab view software. Fig. 3 shows the distribution of the thermocouples at the tested tube section and along it. For measuring friction factor across the tested tubes two 0.1 cm static taps were created at the entrance and exit of the finned section to measure pressure drop across the

finned section. An inverted U-tube manometer is used to measure this pressure difference as the air is the manometric fluid. There is a hole at the top point of the inverted U-tube manometer (not shown in Fig. 1) to overcome the effect of air compressibility.

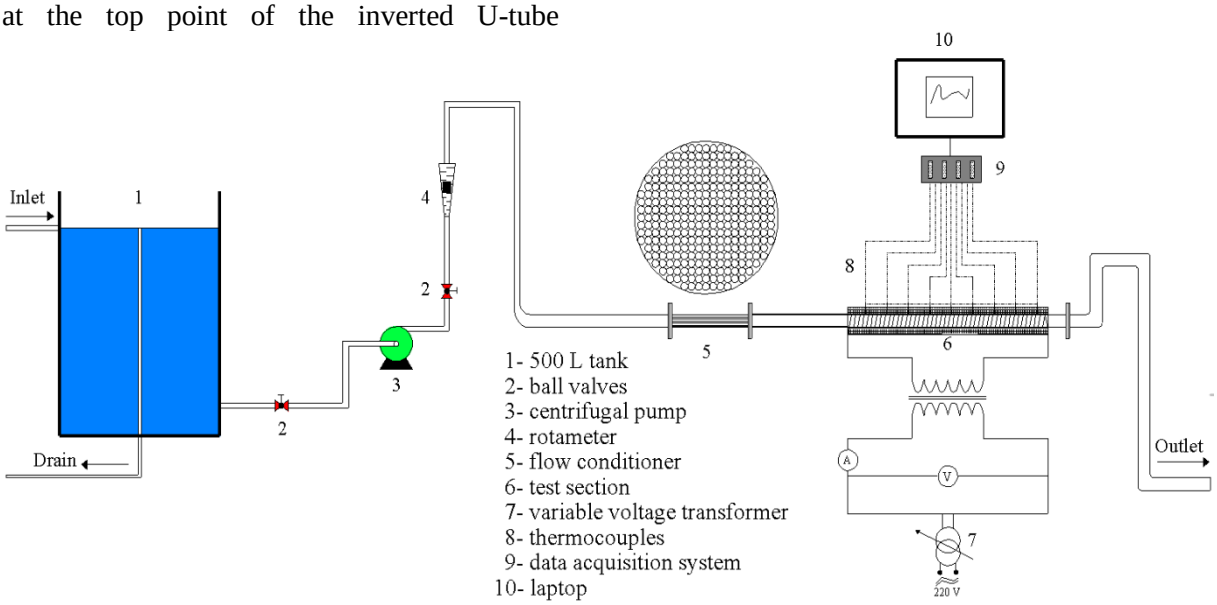

Fig. 1 A schematic layout of the test rig

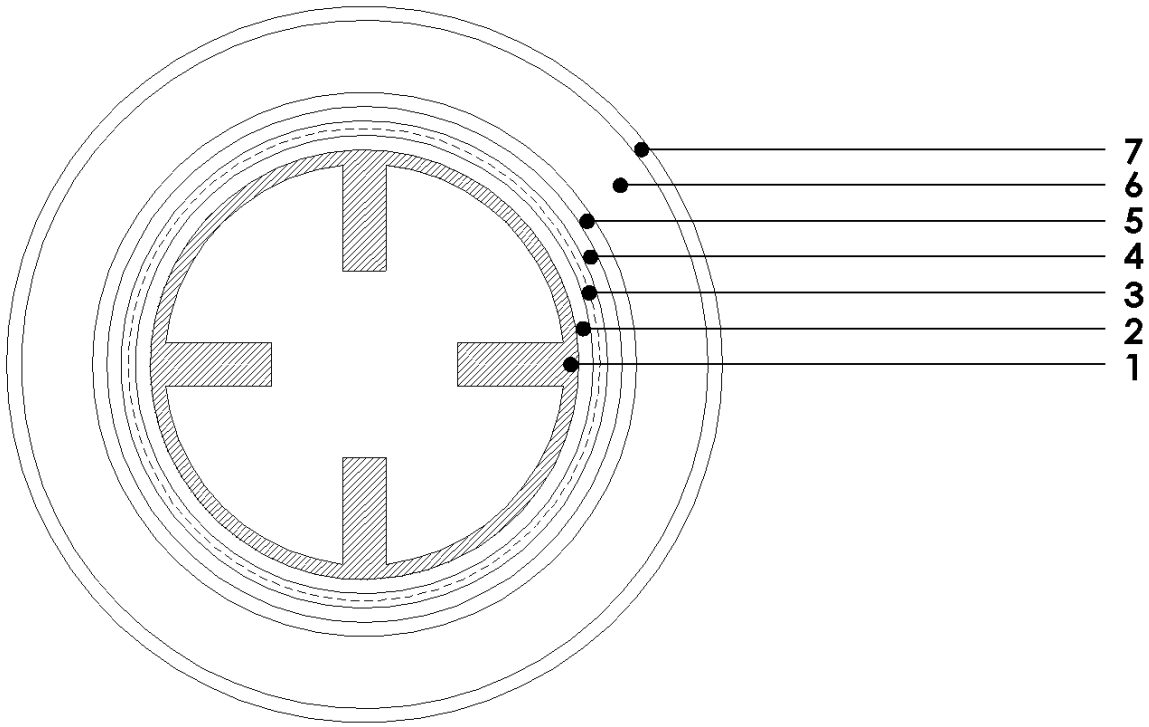

1. test tube
2. asbestos layer
3. electrical heater
4. asbestos layer
5. fiberglass layer
6. fiber ceramic blanket
7. compressed asbestos fiber layer

Fig. 2 A schematic layout of the applied layers on the tested tube

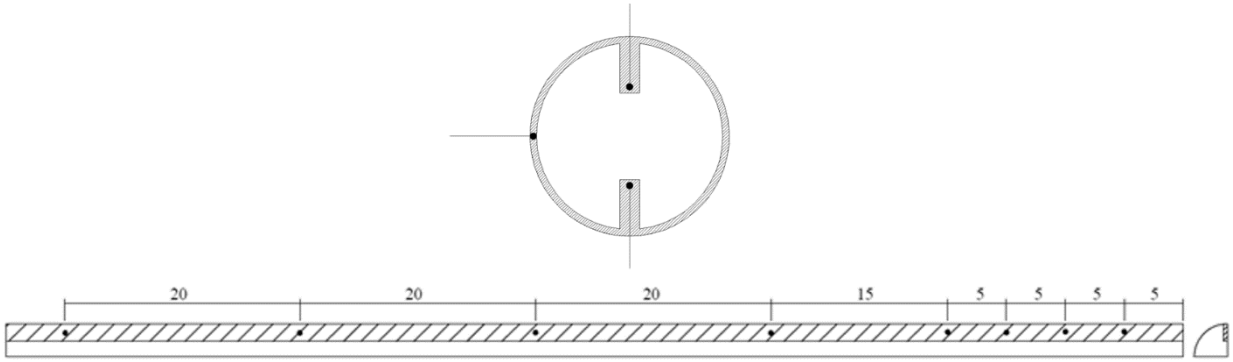

a. N=2

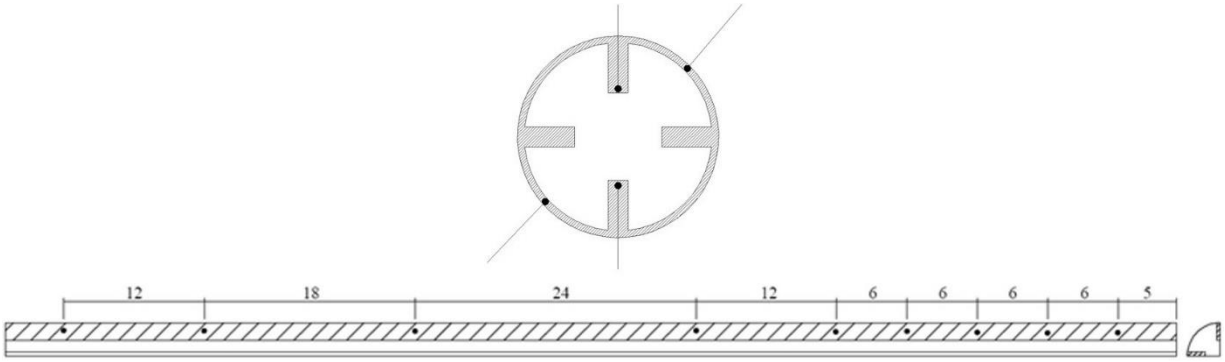

b. N=4

Fig. 3 Thermocouples' distribution positions for the finned tube

2.2 Experimental procedure

The fluid is allowed to circulate through the test section (6) by using a centrifugal pump (3) which works under a nearly constant head. The ball valve (2) is used to control the water flow rate, which is measured by a rotameter (4). The heater is fed by an electricity voltage controller (7), with which the input power can be adjusted. In most experiments, the measurement system is observed to reach steady-state conditions after about 20 minutes. The inlet, outlet, wall, and fin tip temperatures are recorded along the tube using a data acquisition system (9). The pressure difference between the inlet and outlet of the finned section is measured using an inverted U-tube manometer. For the measurement confidence, the experiment is repeated for every reading. The basic measured parameters, besides the geometric dimensions, are utilized to assess the flow field and heat transfer parameters that describe the performance of the internally continuously finned tubes.

2.3 Measurement and uncertainty analysis

After gathering the required experimental data, different characteristic parameters are calculated. The calculations of the heat transfer and fluid flow parameters are defined in Table 1. Also, according to the constant odds method, if a result R is to be calculated by a function $R = R(v_1, v_2, v_2 \dots \dots \dots, v_n)$ from a single set of values of the input data v_i, then the uncertainty in R, As Kline and McClintock [41] proposed, is given by:

$$w_R = \sqrt{\sum_{i=1}^{n} \left(\frac{\partial R}{\partial v_i} w_i \right)^2} \quad (1)$$

where w_i denotes the uncertainty of the i^{th} independent variable. The uncertainty of measured and calculated values during the experiments has been estimated based on the above equation. Table 2 shows samples of the relative uncertainty for different calculated values during the experiments.

Table 1 Calculations of heat transfer and fluid flow parameters

quantity	equation
A_c	$\frac{\pi d^2}{4} - NHt$
d_h	$\frac{4A_c}{\pi d + 2NH}$
A_s	$(\pi d + 2NH)L$
v_f	$\frac{m}{\rho A_c}$
q	$\frac{mC_p(T_o - T_i)}{(\pi d + 2NH)L}$
T_m	$T_i + \frac{q(\pi d + 2NH)x}{mC_p}$
Re	$\frac{\rho v_f d_h}{\mu}$
h	$\frac{q}{T_w - T_m}$
Nu	$\frac{hd_h}{k_{th}}$
f	$\frac{2(\Delta p)d_h}{\rho v_f^2 L}$

Table 2 Relative uncertainty for different calculated experimental parameters

Parameter	Uncertainty %
Re	0.6919
Nu	4.5687
f	3.3958

3. Numerical modeling

3.1 Governing equations and boundary conditions

The present CFD simulation represents an extension study for the experimental results exhibited in the previous section. This numerical study is a three-dimensional steady forced turbulent convection flow study for pure water through continuously finned and finless tubes. The governing equations, including conservation of mass, momentum, and energy with the two equation-based realizable $k-\varepsilon$ model with enhanced wall treatment, are solved using the commercial package solver of Fluent 19, and these equations are explained in detail in [42], and they are as follows:

Continuity equation

$$\frac{\partial}{\partial x_i}\left(\rho v_i\right) = 0 \tag{2}$$

Momentum equation

$$\frac{\partial}{\partial x_j}\left(\rho v_i v_j\right) = -\frac{\partial p}{\partial x_i} + \frac{\partial}{\partial x_j}\left[\mu\left(\frac{\partial v_i}{\partial x_j} + \frac{\partial v_j}{\partial x_i}\right) - \rho\overline{v_i' v_j'}\right] \tag{3}$$

$$-\overline{v_i' v_j'} = 2\frac{\mu_t}{\rho} s_{ij}$$

$$\text{and } s_{ij} = \frac{1}{2}\left(\frac{\partial v_i}{\partial x_j} + \frac{\partial v_j}{\partial x_i}\right) \tag{4}$$

Energy equation

$$\frac{\partial}{\partial x_i}\left(\rho C_p v_i T\right) = -\frac{\partial}{\partial x_i}\left[-k_{th}\frac{\partial T}{\partial x_i} + \rho C_p \overline{v_i' T'}\right] \tag{5}$$

The realizable $k-\varepsilon$ model is chosen for the present simulation since this model showed superior performance for complex flows [42-44], and this model is proposed and explained in detail by Shih et al. [45]. A second-order upwind scheme for convective variables is considered for momentum as well as for the turbulent discretized equations. The mesh near the tube wall and the fin surface area is refined till y^+ near the wall is equal to or less than unity. This will ensure that the boundary layer will be solved quite precisely; especially the viscous sublayer near the wall and this gives a good opportunity to capture the flow fields inside the tube and near the walls. The SIMPLE algorithm with the second-order scheme for pressure is used. The inlet axial velocity is considered uniform. The inlet

temperature and the wall heat flux are uniform. The constant gauge pressure is applied at the outlet boundary condition and the gradients of all the other variables are equal to zero at the outlet. The No-slip boundary condition is applied on all walls of the tube and fins. Fig. 4 shows all boundary conditions of this simulation. The convergence of the discretized equations is achieved when the whole field residuals for all variables fall below 10^{-3}, except for the energy equation, the residual is set to 10^{-6}.

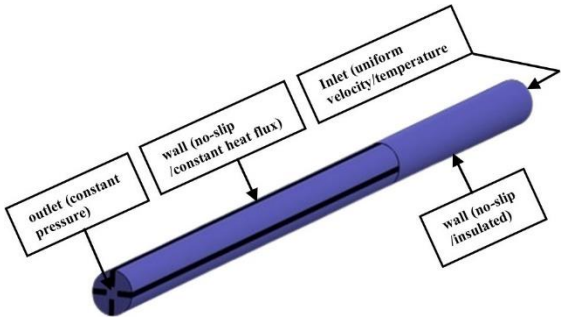

Fig. 4 Boundary conditions for the computational domain

3.2 Grid sensitivity analysis

A grid sensitivity analysis is performed for both cases of finless and continuously finned tubes. Different grid sizes are used in the computations starting from 312480 to 1621236 cells. The grid with 836496 cells is selected for the current simulation as the results become almost constant with the grid number. Fig. 5 shows the generated mesh for the internally continuously finned tubes.

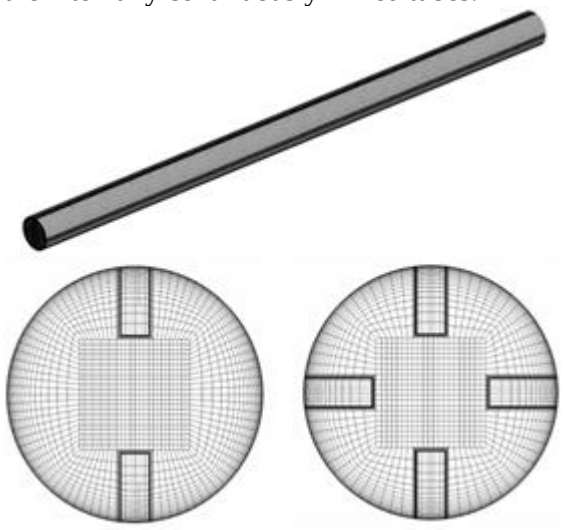

Fig. 5 Computational generated mesh

The mesh independence study based on the average wall temperature, the average fluid temperature at the outlet of the finned section, and the pressure drop across the finned section of the continuously finned tube is conducted. It can be concluded from that study that the percent change in the three parameters from cell number 836496 to 1621236 is less than 1 %. Fig. 6 depicts the mesh independence study for this simulation.

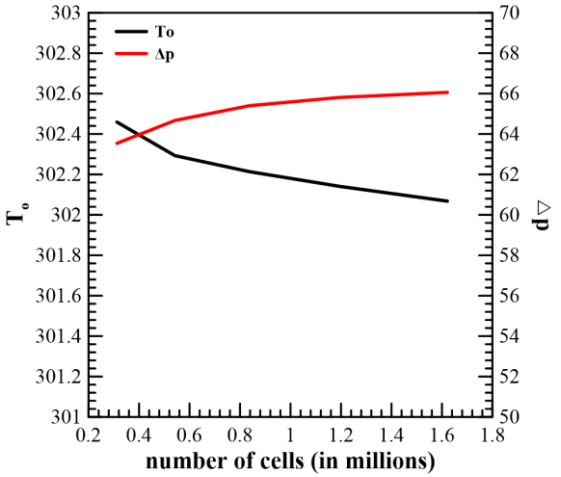

Fig. 6 Mesh independence study

4. Performance evaluation study

To evaluate the performance of the internally continuously finned tubes, a parameter that can be called thermal enhancement factor (TEF) is derived from the first law of thermodynamics. The heat transfer convection and the friction factor are the two main factors on which TEF is built. So, TEF can be defined as follows [46-47]:

$$TEF = \frac{\left(\frac{h}{h_{finless}}\right)}{\left(\frac{f}{f_{finless}}\right)^{\frac{1}{3}}} \quad (6)$$

, Where subscript finless stands for the finless tube. The performance evaluation is calculated at the three widely used constraints; the same mass flow rate, same pumping power, and same pressure drop. Based on the constant properties and the same tube length assumption, the formulations of the three constraints are given as follows:

Same mass flow rate

$$\mathrm{Re}_{finless} = \left(1+\left(\frac{2}{\pi}\right)(N)\left(\frac{H}{d}\right)\right)\mathrm{Re} \qquad (7)$$

Same pressure drop

$$f_{finless}\,\mathrm{Re}^2_{finless} = \frac{\left(1+\left(\frac{2}{\pi}\right)(N)\left(\frac{H}{d}\right)\right)^3}{\left(1-\left(\frac{4}{\pi}\right)(N)\left(\frac{H}{d}\right)\left(\frac{t}{d}\right)\right)^3} f\,\mathrm{Re}^2 \qquad (8)$$

Same pumping power

$$f_{finless}\,\mathrm{Re}^3_{finless} = \frac{\left(1+\left(\frac{2}{\pi}\right)(N)\left(\frac{H}{d}\right)\right)^4}{\left(1-\left(\frac{4}{\pi}\right)(N)\left(\frac{H}{d}\right)\left(\frac{t}{d}\right)\right)^3} f\,\mathrm{Re}^3 \qquad (9)$$

By knowing the Reynolds number and the friction factor for the continuously finned tube, the above equations of the three constraints with the Petukhov correlation [48] for the friction factor of the finless tube can be used to get the Reynolds number for finless tube by which the Nusselt number and friction factor for finless tube can be obtained under the assumed constraint. The TEF value indicates that if it is more than unity, this means that the enhanced tube is thermally beneficial and needs less pumping power compared to the smooth one, under the same conditions, whereas the opposite is true if it is less than unity.

5. Results and discussion

5.1 Experimental results

Fig. 7 shows the variation of the local Nusselt number along the continuously finned tube at different Reynolds numbers for 2 and 4 number of fins. From Fig. 7, it is obvious that the Nusselt number decreases with the distance from the inlet due to the increase in the thermal boundary layer and hence in thermal resistance. Nusselt number rises with the Reynolds number as the thermal boundary layer becomes thinner with the Reynolds number increment. Additionally, from Fig. 7, there is a non-monotonic behavior in some points because some thermocouples may not reach the exact points needed to be measured, and as a result, some temperature values can be out of the main trend. However, this non-monotonic behavior does not affect the mean values.

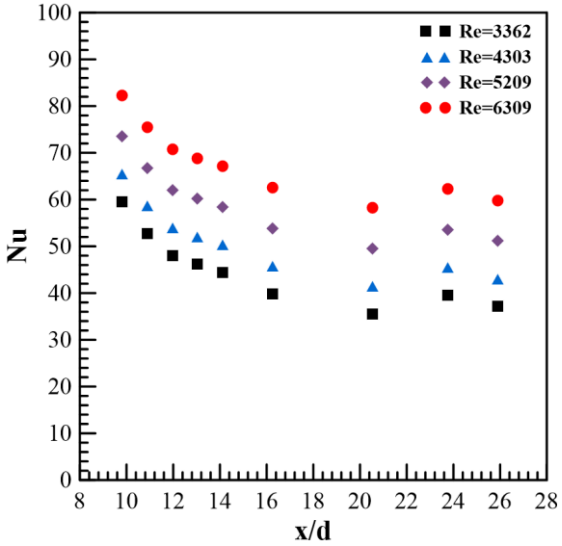

a. N=2

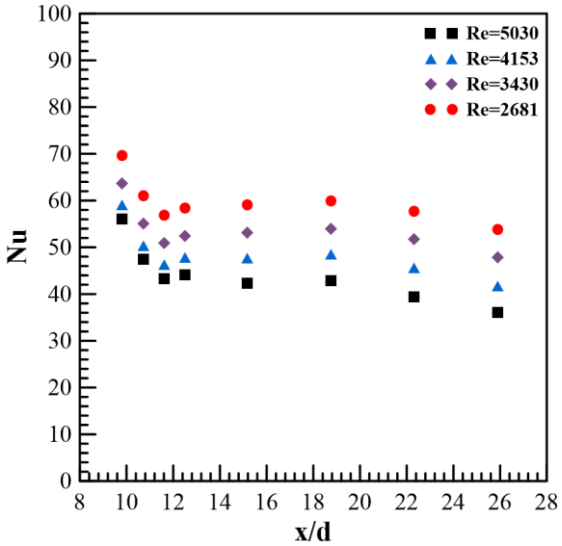

b. N=4

Fig. 7 Variation of local Nusselt number along the finned tubes for different Reynolds number

Fig. 8 and Fig. 9 show the average heat transfer coefficient and friction factor variation, respectively, with mass flowrate for continuously finned tube with 2 and 4 fins, as well as for the finless tube experimental results

which are given by Petukhov correlation [48]. From Fig. 8 and Fig. 9, it is obvious that the heat transfer coefficient for 4 fins is always higher than that for 2 fins due to the larger contact area with fluid particles. Also, this can be attributed to the higher bulk velocity in the case of the continuously finned tube with 4 fins compared to 2 fins due to the smaller flow area. Also, both continuously finned tubes have a higher average heat transfer coefficient compared to the finless one. Furthermore, the friction factor for the continuously finned tube with 4 fins is higher than that of the finless one due to the increase in the internal surface area which is enlarged by adding the fins on the inner surface of the continuously finned tube.

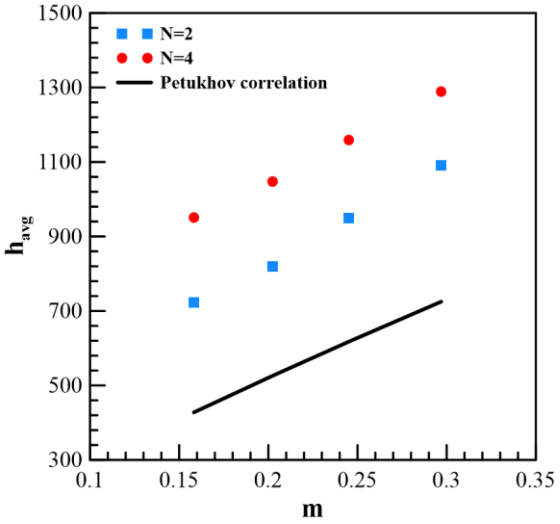

Fig. 8 Average heat transfer coefficient versus mass flowrate for finned tubes and Petukhov [48]

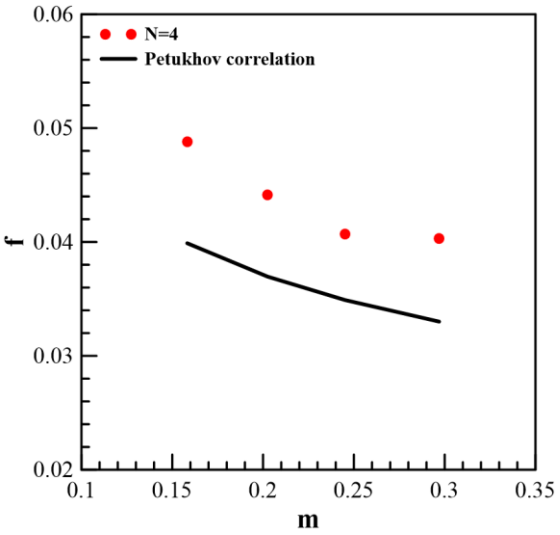

Fig. 9 Average friction factor versus mass flowrate for finned tube (N=4) and Petukhov [48]

5.2 Validation of computational domain

Testing the validation of the developed computational model in this work is carried out in two ways. Firstly, the computational results are compared with experimental data obtained in the current work. Secondly, the computational results are compared with experimental data conducted by El-Sayed et.al [49-50]. Fig. 10 shows a comparison of the present CFD results with the present experimental results for the continuously finned tube, which is equipped with 2 and 4 fins, respectively. As for the continuously finned tube equipped with 2 fins, the maximum percentage error of the average heat transfer coefficient is 4.65 % while for the continuously finned tube equipped with 4 fins, it is 4.5 %. Also, from Fig. 10, it can be seen that the maximum deviation of the numerical results from the experimental ones for the continuously finned tube occurs in the case of the tube fitted with 4 fins and it amounts to 12.58 %. Fig. 11 and Fig. 12 show a comparison of the present CFD results with the experimental results in [49-50]. It can be seen from Fig. 11 that the percentage error of local Nusselt number at any Reynolds number falls under 15.8 %, while from Fig. 12 the percentage error of local dimensionless pressure at any Reynolds number falls under 16.3%. The local dimensionless pressure is defined as follows:

$$-p_{dimensionless} = \frac{2\left(p_i - p_x\right)}{\rho v_f^2} \qquad (10)$$

Also, it can be concluded from Fig. 11 and Fig. 12 that there is a high deviation between the numerical and the experimental results at the inlet of the continuously finned tube models [49-50]. This may be due to the deficiency in the manufacturing of the model and the inlet velocity may be not exactly uniform at the inlet. Table 3 illustrates the average Nusselt number for both numerical and experimental data, which shows that the highest percentage error is 14.16%.

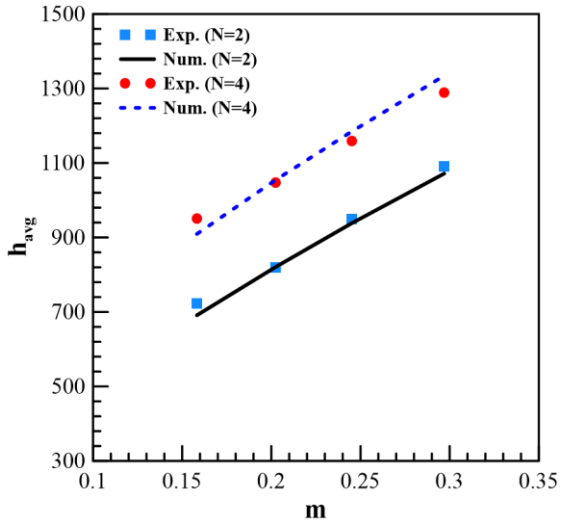

a. heat transfer coefficient

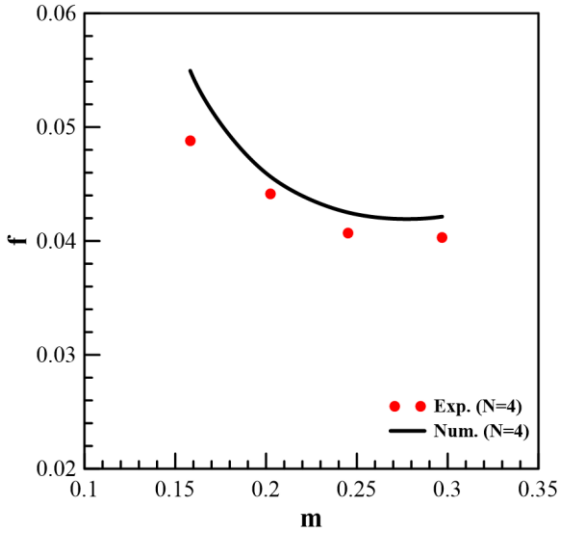

b. friction factor

Fig. 10 Validation with present experimental results

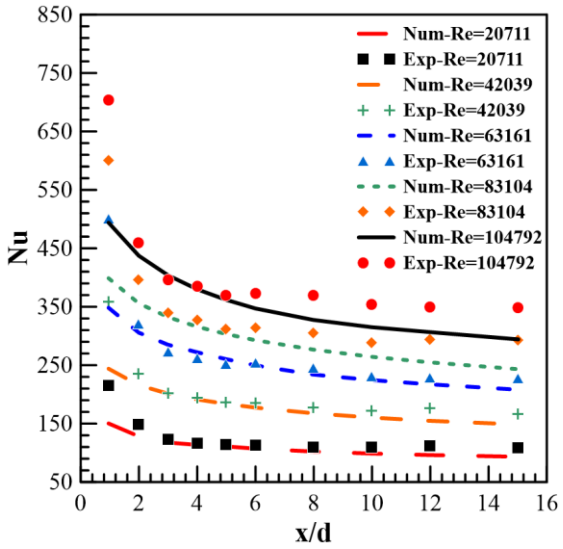

Fig. 11 Local Nusselt number validation with experimental results in [50]

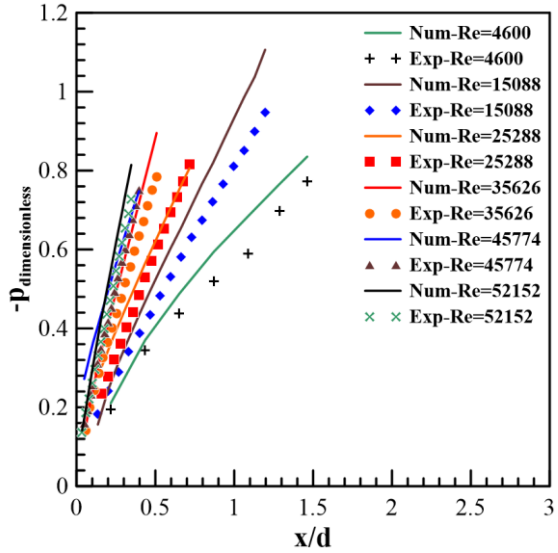

Fig. 12 Local dimensionless pressure validation with experimental results in [49-50]

Table 3 Average Nusselt number validation with experimental data in [49-50]

Re	*Nu* (Num.)	*Nu* (Exp.)	error %
20711	111.87	126.92	13.45
42039	184.54	205.36	11.29
63161	260.53	279.37	7.23
83104	303.83	346.85	14.16
104792	366.78	410.83	12.01

5.3 Numerical results

5.3.1 Geometrical parameters effect

Fin height

Fig. 13 shows the variation of the local heat transfer coefficient for fin height ratio (H/d) of 0.1786, 0.2232, 0.2679, 0.3571, and 0.4018. It can be inferred from Fig. 13 that the heat transfer coefficient grows with increasing fin height ratio. This may be attributed to the increase in heat transfer area between the working fluid and the continuously finned tube walls and the increase in bulk velocity in the finned section. Also, it can be noticed from Fig. 13 that the change rate of heat transfer coefficient at the same local distance ratio (x/d) increases with the fin height ratio because increasing the fin height makes the fin penetrates more fluid layers with lower temperatures while approaching the tube

center, consequently, the temperature difference between the fin surface and the fluid is higher and so does the heat transfer coefficient.

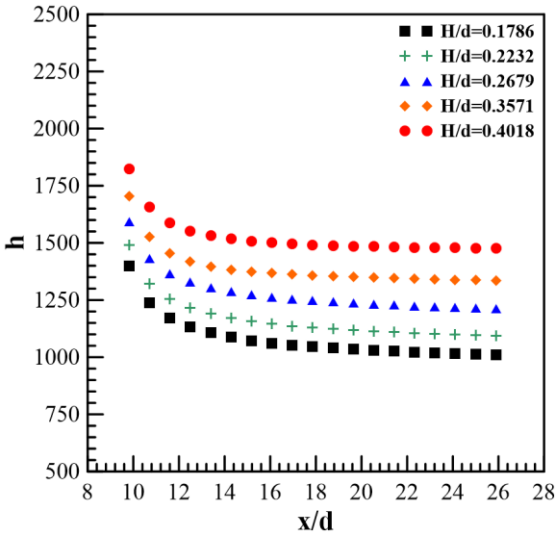

Fig. 13 Local heat transfer coefficient variation along the finned tube with different fin height ratio

Table 4 presents the calculated average values for the Nusselt number, heat transfer coefficient, and friction factor with different fin height ratios. It is clear from Table 4 that the friction factor rises with the fin height ratio due to the increase in contact surface area between the working fluid and the continuously finned tube walls and the disturbance of the flow streams, which are formed by the fin height.

Table 4 The average Nusselt number, heat transfer coefficient, and friction factor variation with fin height ratio (N=4, t/d=0.1071)

H/d	Re	h_{avg}	Nu_{avg}	f
0.1786	5816	1082.90	61.18	0.0385
0.2232	5394	1166.59	59.48	0.0403
0.2679	5030	1283.40	59.32	0.0422
0.3571	4431	1391.61	53.43	0.0463
0.4018	4182	1526.03	53.63	0.0456

Furthermore, it can be seen from Table 4 that the average heat transfer coefficient value and friction factor grow by 40.92 % and 18.44 %, respectively, if the fin height ratio increases from 0.1786 to 0.4018. Furthermore, it can be noticed that the Reynolds number and Nusselt number, which are calculated based on the hydraulic diameter, decrease with fin height ratio due to the reduction in the hydraulic diameter which outweighs the enhancement in heat transfer coefficient.

Number of fins

In Fig. 14, the local heat transfer coefficient is plotted versus the distance ratio for the number of fins of 2, 4, 5, and 6. From Fig. 14, it is clear that the heat transfer coefficient improves with increasing number of fins. This may be attributed to the noticeable growth in heat transfer contact area between the working fluid and the continuously finned tube walls, and the fin walls, too. As well as the increase in the average bulk velocity as the fluid is forced to stream with the same mass flow rate in a smaller flow cross-sectional area. From Fig. 14, it can be noticed that when the number of fins is increased, the rate of rise in heat transfer coefficient declines because increasing the number of fins makes the fins always touch the high-temperature fluid layers only, consequently the temperature difference between the fin surface and the fluid is always low and so does the heat transfer coefficient. Also, when the number of fins is raised, a large part of the main flow becomes stagnant at these fin faces, and many layers of the flow are slow near the fin walls. As a result, the heat transfer rate becomes smaller and so does the heat transfer coefficient.

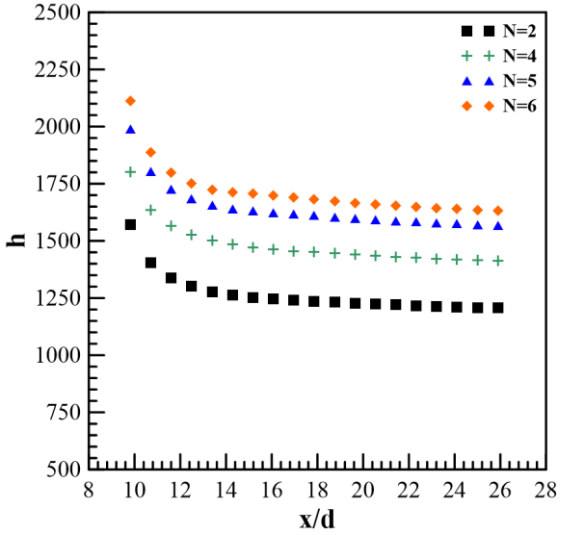

Fig. 14 Local heat transfer coefficient variation along the finned tube with different number of fins

Table 4 presents the calculated average values for the Nusselt number, heat transfer coefficient, and friction factor with different numbers of fins. From Table 5, the average heat transfer coefficient and the friction factor are nearly increased by 35.4 % and 13.51 %, respectively, when the number of fins rises from 2 to 6, but the average Nusselt number, which is calculated based on the hydraulic diameter, decreases with number of fins due to the reduction in the hydraulic diameter which outweighs the enhancement in heat transfer coefficient.

Table 5 The average Nusselt number, heat transfer coefficient, and friction factor variation with number of fins (*H/d*=0.2679, *t/d*=0.1071)

N	*Re*	h_{avg}	Nu_{avg}	*f*
2	8325	1267.64	79.78	0.037
4	6637	1484.30	68.60	0.038
5	6026	1645.13	66.08	0.041
6	5518	1716.44	60.31	0.042

Fin thickness

The local heat transfer coefficient is plotted in Fig. 15 versus the distance ratio for fin thickness ratio (t/d) of 0.0357, 0.0536, 0.0714, 0.0893, and 0.1071. From Fig. 15, it is obvious that the heat transfer coefficient improves with increasing fin thickness, but this improvement is relatively less than that of the fin height effect and the number of fins as the average heat transfer coefficient rises only by 7.82 % when the fin thickness ratio increases from 0.0357 to 0.1071 as shown in Table 6. Also, it can be concluded from Table 6 that the increase in friction factor with fin thickness is very small compared to the effect of fin height and number of fins as the average friction factor rises only by 8.66 % when the fin thickness ratio is increased from 0.0357 to 0.1071. this weak effect is attributed to that the fin thickness does not affect the surface area, but it affects the flow area, which is decreased only by 11.41% when the fin thickness is increased by 200%. Consequently, the increase in heat transfer coefficient is due to the change in the bulk velocity only, which increases only by 11.41%, and not due to the change in the surface area.

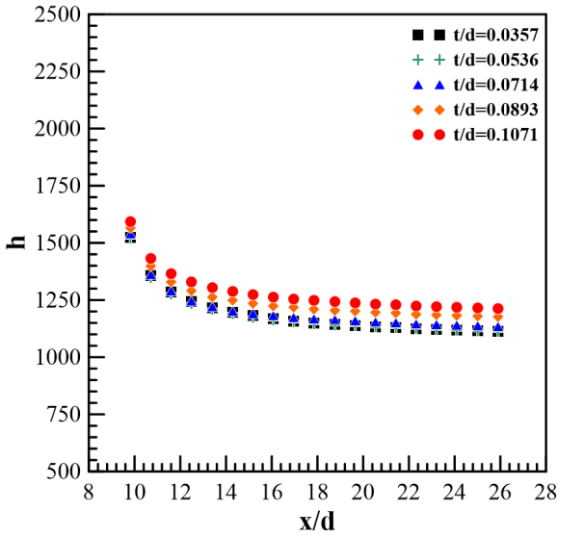

Fig. 15 Local heat transfer coefficient variation along the finned tube with different fin thickness ratio

Table 6 The average Nusselt number, heat transfer coefficient, and friction factor variation with fin thickness ratio (*H/d*=0.2679, *N*=4)

t/d	*Re*	h_{avg}	Nu_{avg}	*f*
0.0357		1190.35	61.29	0.0433
0.0536		1187.25	59.57	0.0432
0.0714	5030	1205.82	58.91	0.0438
0.0893		1246.71	59.26	0.0426
0.1071		1283.40	59.32	0.0422

5.3.2 Dominant geometrical parameter

To investigate whether the fin height or number of fins has the dominant effect on heat transfer for the continuously finned tube, four models are proposed. Fig. 16 shows the dimensions of the four models. All models have the same tube internal diameter and fin thickness (d=5.6 cm, t=0.6 cm) and length (L=100 cm). The first and second models have the same internal surface area. The third and fourth models have the same internal surface area. Fig. 17 represents the local heat transfer coefficient variation along the distance ratio for the four configurations. It is clear from Fig. 17 that the fin height is a more influencing parameter on the thermal performance compared to the number of fins. The continuously finned tube, which is fitted with higher fins and a smaller number of fins, has greater local heat transfer coefficient values

compared to the other finned tube, which is fitted with shorter fins and a greater number of fins, and the difference between the heat transfer coefficient improves when dealing with a higher number of fins. This can be explained as follows: under the same surface area and flow area, the heat transfer mainly occurs due to the temperature difference between the fin surface and the working fluid, and because the longer fins with a smaller number of fins penetrate more fluid layers compared to the shorter fins with a higher number of fins, consequently the temperature difference is high.

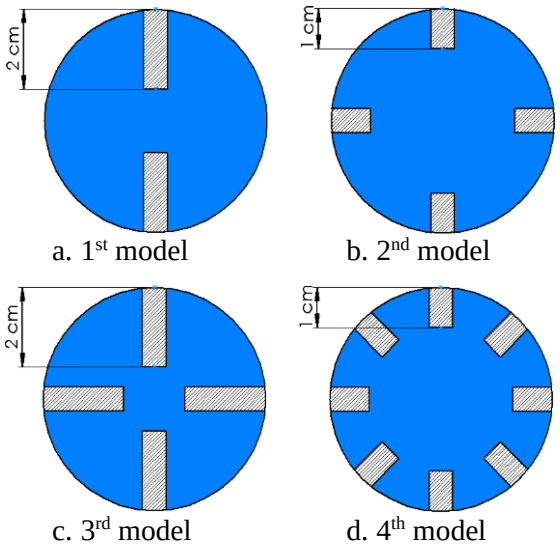

a. 1st model b. 2nd model

c. 3rd model d. 4th model

Fig. 16 Dimensions of the studied four finned tubes with same internal surface area

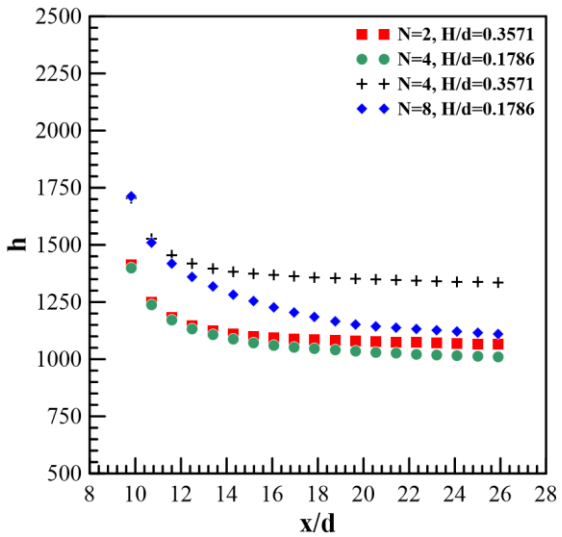

Fig. 17 Local heat transfer coefficient variation along the four tubes with same internal surface area

From Table 7, it is found that the value of the average heat transfer coefficient is enhanced by 3.27 % for the first model compared to the second one, while it is enhanced by 11.7 % for the third model compared to the fourth one. Also, from Table 7, it is found that the friction factor is increased in the case of the tube fitted with higher fins and a smaller number of fins compared to the other tube. Furthermore, it is found that the percentage increase in the friction factor for the first model compared to the second one is 11.17 %, while this increase for the third one is 10.5 % compared to the fourth configuration.

Table 7 The average Nusselt number, heat transfer coefficient, and friction factor for the four tubes with same internal surface area (t/d=0.1071)

H/d	N	Re	h_{avg}	Nu_{avg}	f
0.3571	2	5816	1118.27	63.18	0.0428
0.1786	4		1082.9	61.18	0.0385
0.3571	4	4431	1391.61	53.43	0.0463
0.1786	8		1245.84	47.83	0.0419

5.4 Performance evaluation results

Fig. 18 shows the thermal enhancement factor (TEF) for different fin geometries under various conditions. It can be seen from Fig. 18 that under constant mass flow rate condition, the TEF increases with any fin geometrical parameter, as the TEF is enhanced by 33.27%, 48.64%, and 8.71% if the fin height, number of fins, and fin thickness increase by 125%, 300%, and 200%, respectively. Under constant pressure drop condition, the TEF decreases with any geometrical parameter, as the TEF decreases by 22.89%, 74.53%, and 7.92% if the fin height, number of fins, and fin thickness increase by 125%, 300%, and 200%, respectively. In the case of constant pumping power condition, the TEF hovers around unity for fin height and thickness, and decreases by 23.89% if the number of fins increases from 2 to 8. It can be concluded that the continuously finned tubes are not recommended in case of constant pressure condition, as they need more

pumping power compared to the finless tube under the same heat transfer rate, but they are highly recommended in case of constant mass flow rate, as it can transfer more heat rates compared to the smooth tube and needs the same pumping power. In case of constant pumping power, they are useful with any fin height or thickness, they nearly have the same performance as the smooth tube but are not useful with a greater number of fins.

6. Continuously finned tube correlations

After the discussion of the major parameters that mainly affect the thermal and the hydrodynamic performance of internally continuously finned tubes, the values of heat transfer coefficient, Nusselt number, and friction factor are used to generate three correlations as a function of five independent variables (*Re*, *Pr*, *H/d*, *N*, *t/d*) using the least square method (LSM). Table 8 shows the squared R and the constants for each correlation which states that:

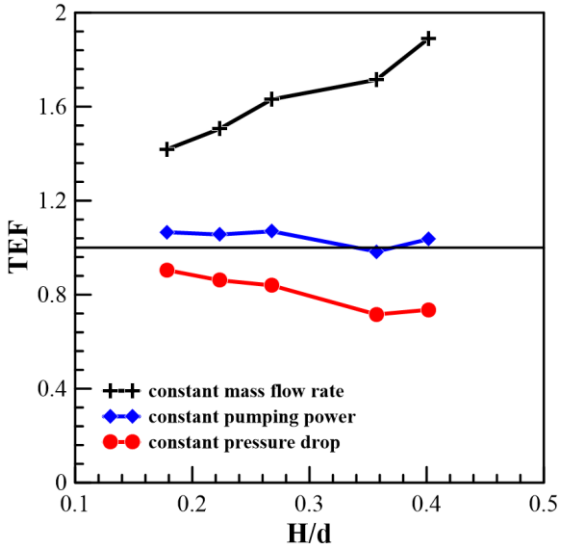

a. H/d

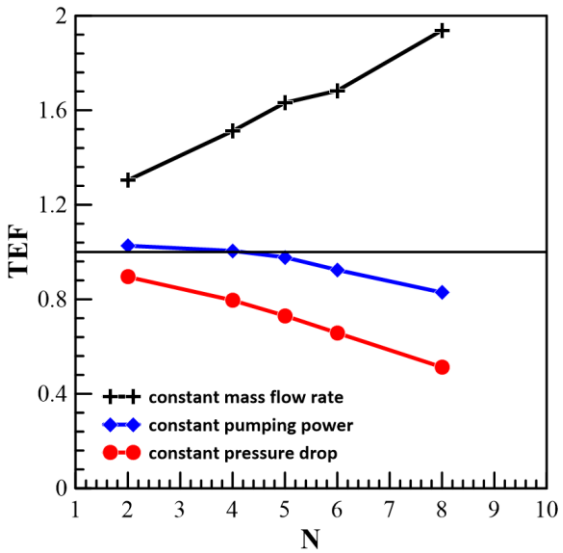

b. N

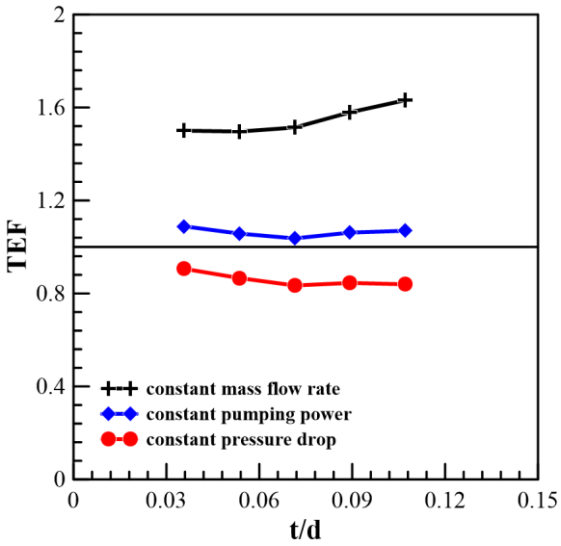

c. t/d

Fig. 18 Performance evaluation for different fin geometry

$$\varphi = c_1 \,\mathrm{Re}^{c_2}\,\mathrm{Pr}^{c_3}\left(\frac{H}{d}\right)^{c_4}(N)^{c_5}\left(\frac{t}{d}\right)^{c_6} \quad (11)$$

Fig. 19 illustrates the Nusselt, heat transfer coefficient, and friction factor values from the current study versus the values generated using the predicted correlations. From Fig. 19 it can be concluded that these correlations can be considered reliable to get the values of the three parameters. Also, for more reliability, the results of the current correlations are compared with the results of the correlations developed by Edwards and Jensen [51] under the same conditions, as shown in Fig. 20. Table 9 shows the dimensions of three different continuously finned tubes for this comparison. It can be concluded from Fig. 20 that the maximum deviation between the results of the current correlations and those of Edwards and Jensen correlations is 17.18% (Tube 1) and 17.77% (Tube 2), in the case of Nusselt number data, while the maximum deviation is 13.7% (Tube 3) in the case of friction factor data. Furthermore, this deviation between the two

developed correlations declines with the Reynolds number. Overall, the developed correlations from the current study can give reliable data for predicting the performance of the continuously finned tubes under the current conditions.

Table 8 Constants of the generated correlations

Eq. const.	φ		
	h_{avg}	Nu_{avg}	f
c_1	2.498	0.2154	0.5940
c_2	0.6682	0.6496	-0.3102
c_3	0.4846	0.0629	0
c_4	0.6762	0.1358	0.1913
c_5	0.5247	0.0264	0.1044
c_6	0.0439	-0.0453	-0.0521
R^2	0.93	0.97	0.76

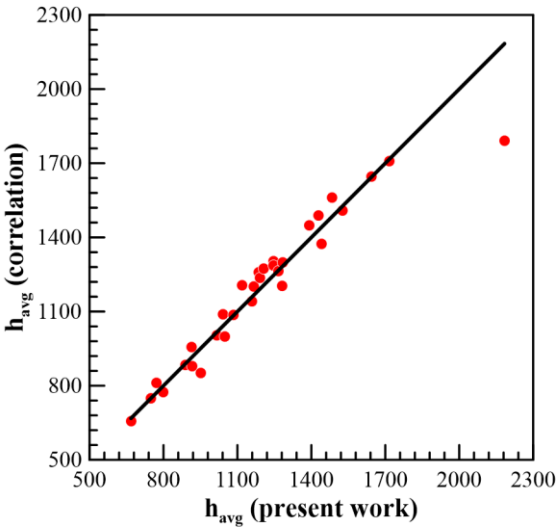

a. heat transfer coefficient

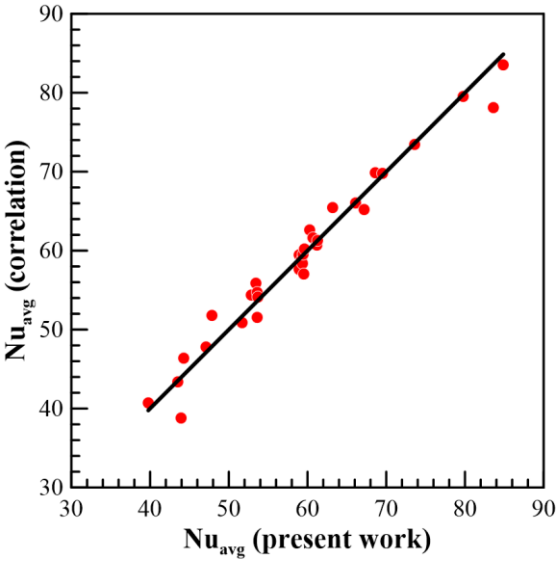

b. Nusselt number

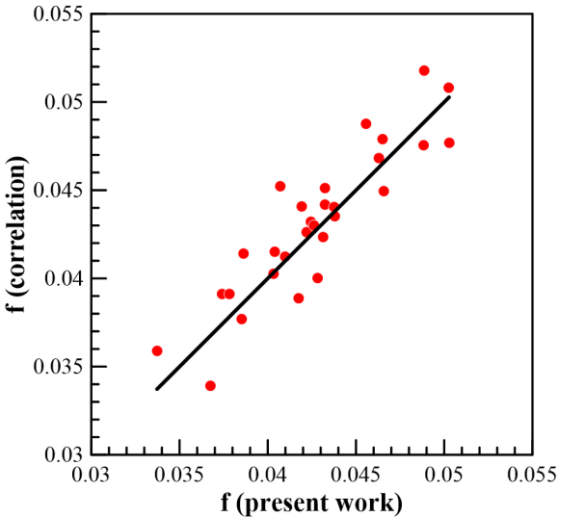

c. friction factor

Fig. 19 The current study and the correlations values comparison

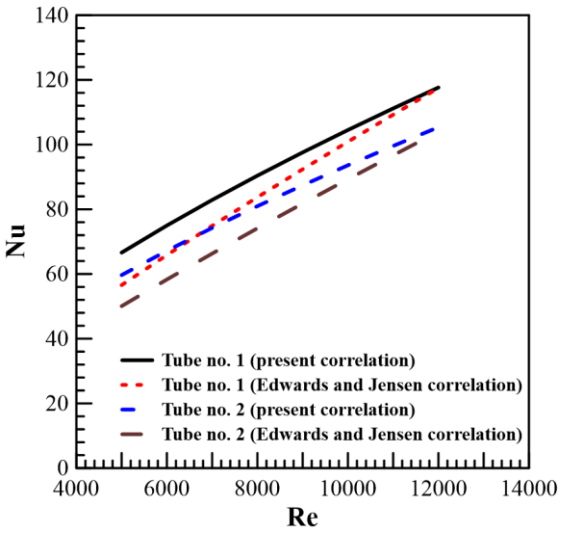

a. Nusselt number

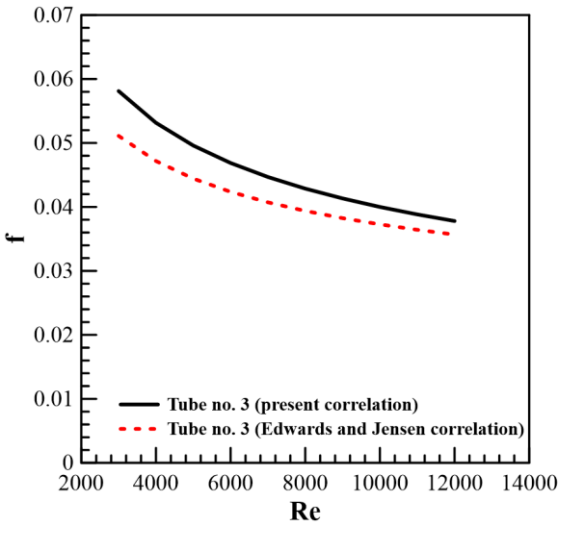

b. friction factor

Fig. 20 Comparison between the current correlations and Edwards and Jensen correlations [51]

Table 9 Dimensions of the tubes used in the correlations comparison

Tube no.	*H/d*	*N*	*t/d*
1	0.4018	4	0.0179
2	0.4018	4	0.0179
3	0.4018	8	0.1071

7. Conclusions

The current paper presents an experimental and numerical study for evaluating the performance of internally finned tubes. The results of this work have led to the following conclusions:

- Heat transfer coefficient increases with Reynolds number, while friction factor always decreases with Reynolds number for all models and both increase remarkably with fin height and number of fins, but inconsiderably with fin thickness. The average heat transfer coefficient and friction factor value rise by 40.92 % and 18.4 %, respectively, if the fin height ratio is increased from 0.1786 to 0.4018, and by 35.4 % and 13.5 %, respectively, if the number of fins is increased from 2 to 6.
- The fin height is the most effective geometrical parameter on the internally finned tube performance compared to the other parameters, as under the same internal area, the continuously finned tubes with a small number of higher fins have a high thermal performance compared to the tubes with a large number of shorter fins.
- Under constant mass flow rate condition, the thermal enhancement factor (TEF) increases with any fin geometrical parameter, as it increases by 33.27%, 48.64%, and 8.71% if the fin height, number of fins, and fin thickness increase by 125%, 300%, and 200%, respectively. While, the thermal enhancement factor decreases with any geometrical parameter under constant pressure drop condition, as it decreases by 22.89%, 74.53%, and 7.92% if the fin height, number of fins, and fin thickness increase by 125%, 300%, and 200%, respectively. In case of constant pumping power condition, it hovers around unity for fin height and thickness, and it decreases with the number of fins, ranging from 2 to 8, by 23.89%.

Future study

Various strategies to further enhance the thermal performance of internally continuously finned tubes can be explored. One way of investigation involves introducing interruptions in the longitudinal fins to promote and increase the turbulence intensity within the flow. By disrupting the flow pattern, these interruptions have the potential to enhance the heat transfer coefficient and improve overall thermal efficiency compared to traditional smooth tubes. In addition, the performance of thermal devices that can be integrated with such tubes can be assessed to be used in modern and current fields related to sustainable energy utilization, such as renewable energy systems, solar energy systems, and industrial cooling and heating processes, or water desalination systems, especially the thermal systems of the water desalination.

Recommendations

Based on the observed performance, the authors recommend further exploration and utilization of internally continuously finned tubes in various heat transfer applications. Their demonstrated advantages over smooth tubes, particularly in terms of enhanced heat transfer performance, position them as promising candidates for heat exchange processes. Also, based on the evaluation study, the authors recommend using the continuously finned tubes over the smooth ones if the amount of mass flow rate flowing through both tubes is the same. But, unfortunately, the use of continuously finned tubes is not recommended as opposed to smooth ones if both tubes are subjected to the same pressure drop across them. Also, if the same pumping power is required for both continuously finned and smooth tubes, the effectiveness of the continuously finned tubes compared to the smooth tubes is enhanced with fin height and thickness, but it is degraded with the number

of fins. Finally, the authors recommended using the generated equations from the current study for the calculations of the heat transfer coefficient, Nusselt number, and friction factor, as these equations are considered reliable in predicting the thermal-hydrodynamic performance of such tubes under different conditions.

CRediT authorship contribution statement

O. H. Salem: Writing –original draft, Visualization, Validation, Software. **Ahmed Hegazy:** Supervision, Review & editing, Investigation, Formal analysis, Data curation. **K. Yousef:** Co-supervision.

Declaration of competing interest

The authors declare that they have no known competing financial interests or personal relationships that could have appeared to influence the work reported in this paper.

Data availability

Data will be made available on request.

References

[1] R. Long, Y.J. Bao, X.M. Huang, W. Liu, Exergy analysis and working fluid selection of organic Rankine cycle for low grade waste heat recovery, Energy 73 (2014) 475-483.

[2] M. Siddique, A.R. Khaled, N.I. Abdulhafiz, A.Y. Boukhary, Recent advances in heat transfer enhancements: a review report, International Journal of Chemical Engineering 2010-1–28, 2010.

[3] R. Gugulothu, K.V.V Reddy, N.S. Somanchi, E.L. Adithya, A review on enhancement of heat transfer techniques, Materials Today: Proceedings 4(2) (2017) 1051-1056.

[4] D. Wang, X. Ling, H. Peng, Simulation of ligament mode breakup of molten slag by spinning disk in the dry granulation process, Applied Thermal Engineering, 84 (2015) 437-447.

[5] H. Peng, Y. Yang, R. Li, X. Ling, Thermodynamic analysis of an improved adiabatic compressed air energy storage system, Applied Energy 183 (2016) 1361-1373.

[6] H. Peng, R. Li, X. Ling, H. Dong, Modeling on heat storage performance of compressed air in a packed bed system, Applied Energy 160 (2015) 1-9.

[7] J. Soria, M.P. Norton, The effect of transverse plate vibration on the mean laminar convective boundary layer heat transfer rate, Experimental Thermal and Fluid Science 4(2) (1991) 226-238.

[8] T. Mizushina, The electrochemical method in transport phenomena, Advances in Heat Transfer 7 (1971) 87-161.

[9] M.M. Ohadi, D.A. Nelson, S. Zia, Heat transfer enhancement of laminar and turbulent pipe flow via corona discharge, International Journal of Heat and Mass Transfer 34(4-5) (1991) 1175-1187.

[10] M. Sheikholeslami, M. Gorji-Bandpy, D.D. Ganji, Review of heat transfer enhancement methods: Focus on passive methods using swirl flow devices, Renewable and Sustainable Energy Reviews 49 (2015) 444-469.

[11] S. Liu, M. Sakr, A comprehensive review on passive heat transfer enhancements in pipe exchangers, Renewable and Sustainable Energy reviews 19 (2013) 64-81.

[12] O. Mahian, E. Bellos, C.N. Markides, R.A. Taylor, A. Alagumalai, L. Yang, S. Wongwises, Recent advances in using nanofluids in renewable energy systems and the environmental implications of their uptake, Nano Energy 86 (2021) 106069.

[13] J. Li, H. Zhai, L. Shi, N. Tan, Y. Zhang, C. Huang, Experimental analysis of convective boiling heat transfer and nanoparticle deposition effect of TiO2-H2O nanofluids in microchannels, Thermal Science and Engineering Progress 47 (2024) 102282.

[14] S. Zeinali, E. Neshat, A. Sarrafzadeh, Comparison of the use of different nanofluids for heat transfer from the outer surface of spiral tubes: energy, exergy, and exergoeconomic (3E) analysis, Case Studies in Thermal Engineering 52 (2023) 103693.

[15] A.H. Alami, M. Ramadan, M. Tawalbeh, S. Haridy, S. Al Abdulla, H. Aljaghoub, M. Ayoub, A. Alashkar, M.A. Abdelkareem, A.G. Olabi, A critical insight on nanofluids for heat transfer enhancement, Scientific Reports 13(1) (2023) 15303.

[16] Z. Said, L.S. Sundar, A.K. Tiwari, H.M. Ali, M. Sheikholeslami, E. Bellos, H. Babar, Recent advances on the fundamental physical phenomena behind stability, dynamic motion, thermophysical properties, heat transport, applications, and challenges of nanofluids, Physics Reports 946 (2021) 1–94.

[17] J. Wang, X. Yang, J.J. Klemeš, K. Tian, T. Ma, B. Sunden, A review on nanofluid stability: preparation and application,

Renewable and Sustainable Energy Reviews 188 (2023) 113854.

[18] S.K. Saha, H. Ranjan, M.S. Emani, A.K. Bharti, Heat transfer enhancement in externally finned tubes and internally finned tubes and annuli, Springer, 2019. (In English)

[19] A. Maji, G. Choubey, Improvement of heat transfer through fins: a brief review of recent developments, Heat Transfer 49(3) (2020) 1658–1685.

[20] E. Tian, Y.L. He, W.Q. Tao, Numerical simulation of finned tube bank across a staggered circular-pin-finned tube bundle, Numerical Heat Transfer, Part A: Applications 68(7) (2015) 737–760.

[21] H.M. Soliman, The effect of fin conductance on laminar heat transfer characteristics of internally finned tubes, The Canadian Journal of Chemical Engineering 59(2) (1981) 251-256.

[22] H.M. Soliman, A. Feingold, Analysis of fully developed laminar flow in longitudinal internally finned tubes, The Chemical Engineering Journal 14(2) (1977) 119-128.

[23] H.M. Soliman, T.S. Chau, A.C. Trupp, Analysis of laminar heat transfer in internally finned tubes with uniform outside wall temperature, ASME 102(4) (1980) 598-604.

[24] Q.W. Wang, M. Lin, M. Zeng, L. Tian, Computational analysis of heat transfer and pressure drop performance for internally finned tubes with three different longitudinal wavy fins, Heat and Mass Transfer 45(2) (2008) 147-156.

[25] Q.W. Wang, M. Lin, M. Zeng, Effect of lateral fin profiles on turbulent flow and heat transfer performance of internally finned tubes, Applied Thermal Engineering 29(14-15) (2009) 3006-3013.

[26] Q. Yang, Y. He, K. Song, Q. Hou, Q. Zhang, X. Wu, Thermal performance improvement of a circular tube-and-fin heat exchanger by ellipsoidal protrusions on fin surfaces, International Journal of Thermal Sciences 196 (2024) 108746.

[27] K. Mohapatra, D.P. Mishra, Effect of fin and tube configuration on heat transfer of an internally finned tube, International Journal of Numerical Methods for Heat and Fluid flow 25(8) (2015) 1978-1999.

[28] K. Mohapatra, R. Mallick, D. Das, S. Pothal, Internal finned tube heat transfer equipment for higher performance, International Journal of Advanced Mechanical Engineering 8 (2018) 199-204.

[29] S.K. Rout, D.N. Thatoi, A.K. Acharya, D.P. Mishra, CFD supported performance estimation of an internally finned tube heat exchanger under mixed convection flow, Procedia Engineering 38 (2012) 585-597.

[30] G. Fabbri, Heat transfer optimization in internally finned tubes under laminar flow conditions, International Journal of Heat and Mass Transfer 41(10) (1998) 1243-1253.

[31] G. Fabbri, Optimum profiles for asymmetrical longitudinal fins in annular ducts, Heat Transfer Engineering 21(2) (2000) 40-52.

[32] G. Fabbri, Effect of viscous dissipation on the optimization of the heat transfer in internally finned tubes, International Journal of Heat and Mass Transfer 47(14-16) (2004) 3003-3015

[33] O. Zeitoun, A.S. Hegazy, Heat transfer for laminar flow in internally finned pipes with different fin heights and uniform wall temperature, Heat and Mass Transfer 40(3) (2004) 253-259.

[34] K.A. Yousef, O.H. Salem, A.S. Hegazy, Numerical analysis of turbulent flow in a 3-d horizontal finned tube with uniform heat flux, Engineering Research Journal 45(2) (2022) 181-192.

[35] T. Tabassum, M. Hasan, L. Begum, Thermal energy storage through melting of a commercial phase change material in an annulus with radially divergent longitudinal fins, International Journal of Thermofluid Science and Technology 7(1) (2020) 20070102.

[36] X.Y. Zhang, Y.T. Ge, P.Y. Lang, Experimental investigation and CFD modelling analysis of finned-tube PCM heat exchanger for space heating, Applied Thermal Engineering 244 (2024) 122731.

[37] M. Heydari, D. Toghraie, O.A. Akbari, The effect of triangular porous medium and non-Newtonian nanofluid on flow and heat transfer properties in a constant-flux microchannel, Thermal Science and Engineering Progress 2 (2017) 140-150.

[38] K. Sun, Y. Zhang, C. Gao, K. Song, Q. Hou, M. Su, W. Dang, Thermal performance augmentation of inner spiral finned tube for linear fresnel solar reflector, Thermal Science and Engineering Progress 49 (2024) 102483.

[39] H.A. Hassan, V.M. Hameed, An implementation investigation on hydrothermal behavior of heat exchanger with a novel finned tube designed, Arabian Journal for Science and Engineering (2024) 1-10.

[40] J. Guo, B. Yang, Y. Li, X. Yang, Y.L. He, B. Sundén, Thermal energy storage characteristics of finned tubes with different

gradients of fin heights, Numerical Heat Transfer 85(6) (2024) 845-874.
[41] S.J. Kline, F.A. McClintock, Describing uncertainties in single-sample experiments, Mechanical Engineering 75(1) (1953) 3-8.
[42] H.K. Versteeg, W. Malalasekera, An introduction to computational fluid dynamics: the finite volume method, Pearson Education Limited, Harlow, England, 2007. (In English)
[43] M. Ahsan, Numerical analysis of friction factor for a fully developed turbulent flow using k–ε turbulence model with enhanced wall treatment, Beni-Suef University Journal of Basic and Applied Sciences 3(4) (2014) 269-277.
[44] Z. Liu, Y. Yue, L. She, G. Fan, Numerical analysis of turbulent flow and heat transfer in internally finned tubes, Frontiers in Energy Research 7 (2019) 64.
[45] T.H. Shih, W.W. Liou A. Shabbir Z. Yang, J. Zhu, A new k-ε eddy viscosity model for high Reynolds number turbulent flows, Computers and Fluids 24(3) (1995) 227-238.
[46] Y. Fang, I.B. Mansir, A. Shawabkeh, A. Mohamed, F. Emami, Heat transfer, pressure drop, and economic analysis of a tube with a constant temperature equipped with semi-circular and teardrop-shaped turbulators, Case Studies in Thermal Engineering 33 (2022) 101955.
[47] M. Sun, M. Zeng, Investigation on turbulent flow and heat transfer characteristics and technical economy of corrugated tube, Applied Thermal Engineering 129(1) (2018) 1-11.
[48] B.S. Petukhov, Heat transfer and friction in turbulent pipe flow with variable physical properties, Advances in Heat Transfer 6(C) (1970) 503-564.
[49] S.A. El-Sayed, S.A. El-Sayed, M.E. Abdel-Hamid, M.M. Sadoun, Experimental study of turbulent flow inside a circular tube with longitudinal interrupted fins in the stream wise direction, Experimental Thermal and Fluid Science 15(1) (1997) 1-15.
[50] S. El-Sayed, S. El-Sayed, M. Saadoun, Experimental study of heat transfer to flowing air inside a circular tube with longitudinal continuous and interrupted fins, Journal of Electronics Cooling and Thermal Control 2(1) (2012) 1-16.
[51] DP. Edwards, M. K. Jensen, An investigation of turbulent flow and heat transfer in longitudinally finned tubes, Heat Transfer Laboratory Report HTL-18, Rensselaer Polytechnic Institute, Troy, NY, 1994.